# The Dual-Targeted Purple Acid Phosphatase Isozyme AtPAP26 Is Essential for Efficient Acclimation of Arabidopsis to Nutritional Phosphate Deprivation[1,2][W][OA]

**Brenden A. Hurley[3,4], Hue T. Tran[3], Naomi J. Marty, Joonho Park, Wayne A. Snedden, Robert T. Mullen, and William C. Plaxton***

Department of Biology (B.A.H., H.T.T., J.P., W.A.S., W.C.P.) and Department of Biochemistry (W.C.P.), Queen's University, Kingston, Ontario, Canada K7L 3N6; and Department of Molecular and Cellular Biology, University of Guelph, Guelph, Ontario, Canada N1G 2W1 (N.J.M., R.T.M.)

Induction of intracellular and secreted acid phosphatases (APases) is a widespread response of orthophosphate (Pi)-starved (−Pi) plants. APases catalyze Pi hydrolysis from a broad range of phosphomonoesters at an acidic pH. The largest class of nonspecific plant APases is comprised of the purple APases (PAPs). Although the biochemical properties, subcellular location, and expression of several plant PAPs have been described, their physiological functions have not been fully resolved. Recent biochemical studies indicated that AtPAP26, one of 29 PAPs encoded by the Arabidopsis (*Arabidopsis thaliana*) genome, is the predominant intracellular APase, as well as a major secreted APase isozyme up-regulated by −Pi Arabidopsis. An *atpap26* T-DNA insertion mutant lacking *AtPAP26* transcripts and 55-kD immunoreactive AtPAP26 polypeptides exhibited: (1) 9- and 5-fold lower shoot and root APase activity, respectively, which did not change in response to Pi starvation, (2) a 40% decrease in secreted APase activity during Pi deprivation, (3) 35% and 50% reductions in free and total Pi concentration, respectively, as well as 5-fold higher anthocyanin levels in shoots of soil-grown −Pi plants, and (4) impaired shoot and root development when subjected to Pi deficiency. By contrast, no deleterious influence of AtPAP26 loss of function occurred under Pi-replete conditions, or during nitrogen or potassium-limited growth, or oxidative stress. Transient expression of *AtPAP26-mCherry* in Arabidopsis suspension cells verified that AtPAP26 is targeted to the cell vacuole. Our results confirm that AtPAP26 is a principal contributor to Pi stress-inducible APase activity, and that it plays an important role in the Pi metabolism of −Pi Arabidopsis.

Orthophosphate (Pi) is an essential plant macronutrient required for many pivotal metabolic processes such as photosynthesis and respiration. However, the massive use of Pi fertilizers in agriculture demonstrates how the free Pi level of many soils is suboptimal for plant growth. The world's reserves of rock phosphate, our major source of Pi fertilizers, are projected to be depleted by the end of this century (Vance et al., 2003). Furthermore, Pi runoff from fertilized fields into nearby surface waters results in environmentally destructive processes such as aquatic eutrophication and blooms of toxic cyanobacteria. Effective biotechnological strategies are needed to engineer Pi-efficient transgenic crops to ensure agricultural sustainability and a reduction in Pi fertilizer overuse. This necessitates a detailed understanding of Pi-starvation-inducible (PSI) gene expression and the complex morphological, physiological, and biochemical adaptations of Pi-deficient (−Pi) plants.

A well-documented component of the plant Pi stress response is the up-regulation of intracellular and secreted acid phosphatases (APases; E.C. 3.1.3.2) that catalyze the hydrolysis of Pi from various phosphate monoesters and anhydrides in the acidic pH range (Tran et al., 2010a). APase induction by −Pi plants has been correlated with de novo APase synthesis in several species, including white lupin (*Lupinus albus*), tomato (*Solanum lycopersicum*), and Arabidopsis (*Arabidopsis thaliana*; Miller et al., 2001; Bozzo et al., 2006; Veljanovski et al., 2006; Bozzo and Plaxton, 2008; Tran and Plaxton, 2008). The probable function of intracellular APases is to recycle Pi from expendable intracel-

[1] This work was supported by grants from the Natural Sciences and Engineering Research Council of Canada (NSERC) and Queen's Research Chairs program (to W.C.P.), and from NSERC and the University of Guelph Research Chairs program (to R.T.M.). B.A.H. and H.T.T. were the beneficiaries of NSERC postgraduate scholarships.

[2] This article is dedicated to the memory of the late Professor David T. Canvin, a Queen's University colleague and eminent plant physiologist.

[3] These authors contributed equally to the article.

[4] Present address: University of Toronto, Department of Cell and Systems Biology, 25 Harbord Street, Toronto, Ontario, Canada M5S 3G5.

* Corresponding author; e-mail plaxton@queensu.ca.

The author responsible for distribution of materials integral to the findings presented in this article in accordance with the policy described in the Instructions for Authors (www.plantphysiol.org) is: William C. Plaxton (plaxton@queensu.ca).

[W] The online version of this article contains Web-only data.

[OA] Open Access articles can be viewed online without a subscription.

www.plantphysiol.org/cgi/doi/10.1104/pp.110.153270

lular organophosphate pools. This is accompanied by a marked reduction in cytoplasmic phosphate metabolites during extended Pi stress (Bozzo and Plaxton, 2008; Tran et al., 2010a). Secreted APases belong to a group of PSI phosphohydrolases believed to mobilize Pi from the external organophosphates prevalent in many soils (Vance et al., 2003; Bozzo and Plaxton, 2008). Molecular analyses of PSI transcripts and proteins have hinted at complex control of plant APase gene expression. Pi deprivation induces temporal and tissue-specific expression of PSI APase isozymes (Haran et al., 2000; Wu et al., 2003; Zimmerman et al., 2004; Bozzo et al., 2006) and the concomitant down-regulation of other APases (Misson et al., 2005). The transcription factors PHR1, WRKY75, and ZAT6 have been implicated in the control of Arabidopsis PSI APases (Rubio et al., 2001; Devaiah et al., 2007a, 2007b), while posttranscriptional mechanisms appear to be essential for the up-regulation of the purple APase (PAP) AtPAP26 during Pi stress (Veljanovski et al., 2006; Tran and Plaxton, 2008; Tran et al., 2010b). In contrast, Pi resupply to −Pi plants rapidly represses PSI APase genes (del Pozo et al., 1999; Müller et al., 2004; Veljanovski et al., 2006) while inducing proteases that target PSI-secreted APases (Bozzo et al., 2004b). Further characterization of PSI APases is required to define the molecular mechanisms underlying this archetypical plant response to Pi starvation, as well as to identify additional targets for biotechnological improvement of crop Pi acquisition.

A variety of intracellular and secreted APases up-regulated by −Pi plants have been characterized as purple APases (PAPs), which represent a specific APase class characterized by a bimetallic active site that endows them with a pink or purple color in solution (del Pozo et al., 1999; Bozzo et al., 2002, 2004a, 2006; Veljanovski et al., 2006; Tran et al., 2010b). Although mammals contain a pair of PAP-encoding genes, vascular plant PAPs belong to a large multigene family. Li and coworkers (2002) classified 29 putative PAP genes in Arabidopsis, several of which appear to respond to Pi deficiency. Apart from functioning as nonspecific APases, several PSI plant PAPs (including AtPAP17 and AtPAP26) exhibit alkaline peroxidase activity, indicating their potential alternative role in the metabolism of reactive oxygen species (del Pozo et al., 1999; Bozzo et al., 2002, 2004a; Veljanovski et al., 2006). Moreover, AtPAP17 was induced by oxidative stress (del Pozo et al., 1999) and ectopic expression of a soybean (*Glycine max*) mitochondrial PAP (GmPAP3) conferred increased resistance to oxidative stress in transgenic Arabidopsis (Francisca Li et al., 2008). It is therefore important to determine the physiological roles of the various plant PAPs and which of their dual enzymatic activities are functional in −Pi plants.

The aim of this study was to build upon biochemical analyses indicating that AtPAP26 is the predominant intracellular (vacuolar; Veljanovski et al., 2006), as well as a major secreted APase isozyme up-regulated by −Pi Arabidopsis (Tran and Plaxton, 2008; Tran et al., 2010b). Although the purified intracellular versus secreted AtPAP26 isoforms of −Pi Arabidopsis shared an identical transit peptide cleavage site, they showed significant differences in the nature of the oligosaccharide side chains that are posttranslationally attached to this glycoprotein; glycosylation was therefore suggested to play an important role in the differential targeting of AtPAP26 during Pi stress (Tran et al., 2010b). In this study, we sought to test the hypothesis that AtPAP26 plays an important Pi-scavenging role in Arabidopsis during Pi stress. This was done by taking advantage of the publicly available T-DNA-tagged insertional mutagenized populations of Arabidopsis (Alonso et al., 2003). We identified and characterized a null *atpap26* allele that abrogated *AtPAP26* expression. This was correlated with the elimination of PSI intracellular APase activity, as well as a significant reduction in secreted APase activity during Pi deprivation. The *atpap26* mutant demonstrated impaired development and decreased free and total Pi levels when exposed to Pi deficiency. Our results establish a firm role for AtPAP26 in facilitating the acclimation of Arabidopsis to suboptimal Pi nutrition.

## RESULTS AND DISCUSSION

### Identification and Validation of an *atpap26* Mutant Allele

To assess the contribution of AtPAP26 to intracellular and secreted APase activity during Pi deficiency, as well as its impact on the phenotype of +Pi versus −Pi Arabidopsis, a T-DNA insertion line was identified in the Salk collection (Salk_152821; Alonso et al., 2003). The T-DNA insert was predicted to be located in the seventh intron of the *AtPAP26* gene (locus At5g34850; Fig. 1A) and this position was verified by PCR screening of genomic DNA (gDNA) using an *AtPAP26* gene-specific primer and a T-DNA left border primer (Fig. 1B). Homozygosity of the T-DNA mutant was confirmed by PCR of gDNA using *AtPAP26*-specific primers (Fig. 1B). T-DNA insert number was assessed by Southern blotting of gDNA that had been digested with *Eco*RI, *Hin*dIII, or *Sac*I. Each restriction enzyme cleaves a single digestion site within the integrated *pBIN-pROK2* vector. All digestions yielded a single strongly hybridizing band (Fig. 1C), indicating a single T-DNA insertion site.

The impact of the T-DNA insertion on *AtPAP26* expression was investigated by performing reverse transcription (RT)-PCR using primer pairs to amplify cDNA sequences flanking the second intron of *AtPAP26* (Fig. 1A). AtPAP26 transcripts were observed in shoot and root mRNA isolated from wild-type Columbia-0 (Col-0), but not *atpap26* mutant plants (Fig. 2A). *AtPAP12*, *AtPAP17*, and *AtPPCK1* (encodes phospho*enol*pyruvate [PEP] carboxylase protein kinase1) were employed as positive controls as their transcript levels are markedly increased in −Pi Arabidopsis (del Pozo et al., 1999; Haran et al., 2000;

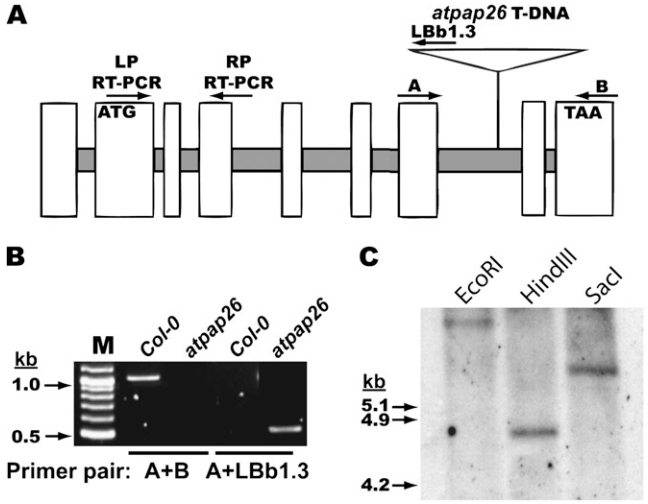


**Figure 1**. Confirmation of T-DNA insert location and copy number in an *atpap26* T-DNA insertional mutant. A, Schematic representation of *AtPAP26* gene (At5g34850); white boxes and solid lines represent exons and introns, respectively. T-DNA insertion location is indicated by *atpap26* T-DNA, while arrows represent primers used for RT-PCR and genotyping. B, Assessment of T-DNA location and homozygosity of mutants via PCR-based screening of gDNA template isolated from +Pi seedlings. PCR products were amplified from Col-0 and *atpap26* gDNA in a 30-cycle PCR reaction containing the indicated primers. The letter M denotes a 100-bp ladder for confirmation of product size. C, Analysis of T-DNA insert number by Southern-blot analysis of *atpap26* gDNA probed with *NPTII*. Arrows indicate the base pair length of *Eco*RI and *Hin*dIII digested phage λ-DNA markers labeled with dig (Roche).

Li et al., 2002; Tran and Plaxton, 2008; Gregory et al., 2009; Tran et al., 2010b). All of these Pi-responsive control transcripts showed a similar induction in −Pi *atpap26* mutant and wild-type Col-0 seedlings (Fig. 2A), indicating that the mutant is unimpaired in Pi-starvation signaling.

Consistent with previous studies (Veljanovski et al., 2006; Tran and Plaxton, 2008; Tran et al., 2010b), the amount of 55-kD AtPAP26 immunoreactive polypeptides were about 2-fold greater in root or shoot extracts from the −Pi relative to +Pi Col-0 seedlings (Fig. 2B), and this was paralleled by the pronounced accumulation of secreted AtPAP26 polypeptides in the media of −Pi Col-0 seedlings (Fig. 3). By contrast, immunoblotting of clarified shoot or root extracts, or secretome proteins of the +Pi or −Pi *atpap26* mutant failed to reveal any immunoreactive AtPAP26 subunits (Figs. 2B and 3), whereas the up-regulation and secretion of 60-kD AtPAP12 polypeptides during Pi stress was unaffected (Fig. 3). Therefore, *atpap26* defines a null allele of *AtPAP26*, with abrogated expression of *AtPAP26* transcript and protein. Results of Fig. 2A corroborate previous studies of Arabidopsis suspension cells and seedlings, documenting the up-regulation of intracellular and secreted AtPAP26 polypeptides in response to Pi starvation, without concomitant changes in *AtPAP26* transcript abundance (Veljanovski et al., 2006; Tran and Plaxton, 2008; Tran et al., 2010b). Recent proteomic studies have observed a variety of intracellular and secreted proteins that are also controlled posttranscriptionally at the level of protein accumulation in Arabidopsis, maize (*Zea mays*), and rice (*Oryza sativa*) plants responding to changes in environmental Pi availability (Fukuda et al., 2007; Li et al., 2008; Tran and Plaxton, 2008). In contrast to AtPAP26, the up-regulation of Arabidopsis PAPs such as *AtPAP12* and *AtPAP17* during Pi deprivation appears to be mainly controlled at the transcriptional level (del Pozo et al., 1999; Haran et al., 2000; Li et al., 2002; Tran and Plaxton, 2008; Tran et al., 2010b; Fig. 2A). As AtPAP12 is secreted by −Pi Arabidopsis suspension cells and seedlings (along with AtPAP26) it is expected to play an extracellular Pi-scavenging role (Fig. 3B; Tran and Plaxton, 2008; Tran et al., 2010b). *AtPAP17* (formerly known as *ACP5*) transcripts also accumulate in response to oxidative or salt stress, similar to *GmPAP3* (del Pozo et al., 1999; Francisca Li et al., 2008). AtPAP17 may thus function to detoxify reactive oxygen species during general stress rather than play a significant Pi remobilization and scavenging role in −Pi Arabidopsis.

### AtPAP26 Is the Predominant Intracellular and a Major Secreted APase Isozyme Up-Regulated by −Pi Arabidopsis

Pi deprivation of Col-0 seedlings resulted in 2- to 3-fold increases in shoot, root, and secreted APase activities (Figs. 2C and 3), as previously reported (Zakhleniuk et al., 2001; Veljanovski et al., 2006; Tran and Plaxton, 2008; Tran et al., 2010b). However, the −Pi *atpap26* mutant exhibited 9- and 5-fold lower shoot and root APase activities, respectively (Fig. 2C), as well as a 40% reduction in secreted APase activity relative to Col-0 (Fig. 3). It is notable that no increase in intracellular APase activity was detected in response to Pi starvation of the *atpap26* mutant (Fig. 2C). APase assays employing 5 mM *para*-nitrophenol-P (*p*NPP) rather than 5 mM PEP as the substrate were also performed with shoot and root extracts of −Pi *atpap26* and Col-0 seedlings. Consistent with the PEP-based assays (Fig. 2C), extracts from −Pi shoots and roots of *atpap26* seedlings, respectively, exhibited about 4- and 6-fold lower *p*NPP-hydrolyzing activity relative to Col-0 controls (shoots = 65 ± 7 and 265 ± 20 nmol pNPP hydrolyzed $min^{-1}$ $mg^{-1}$ protein, respectively; roots = 35 ± 3 and 202 ± 33 nmol pNPP hydrolyzed $min^{-1}$ $mg^{-1}$ protein, respectively; means ± SE of $n = 4$ biological replicates).

Clarified extracts of −Pi shoots were also resolved by nondenaturing PAGE and subjected to in-gel APase activity staining using β-naphthyl-*P* as the substrate, and parallel immunoblotting with anti-AtPAP26 immune serum (Fig. 2D). Shoot extracts of −Pi Col-0 yielded several APase activity-staining bands on nondenaturing gels, in agreement with previous results (Tomscha et al., 2004). However, an abundant high molecular mass APase activity-staining band that

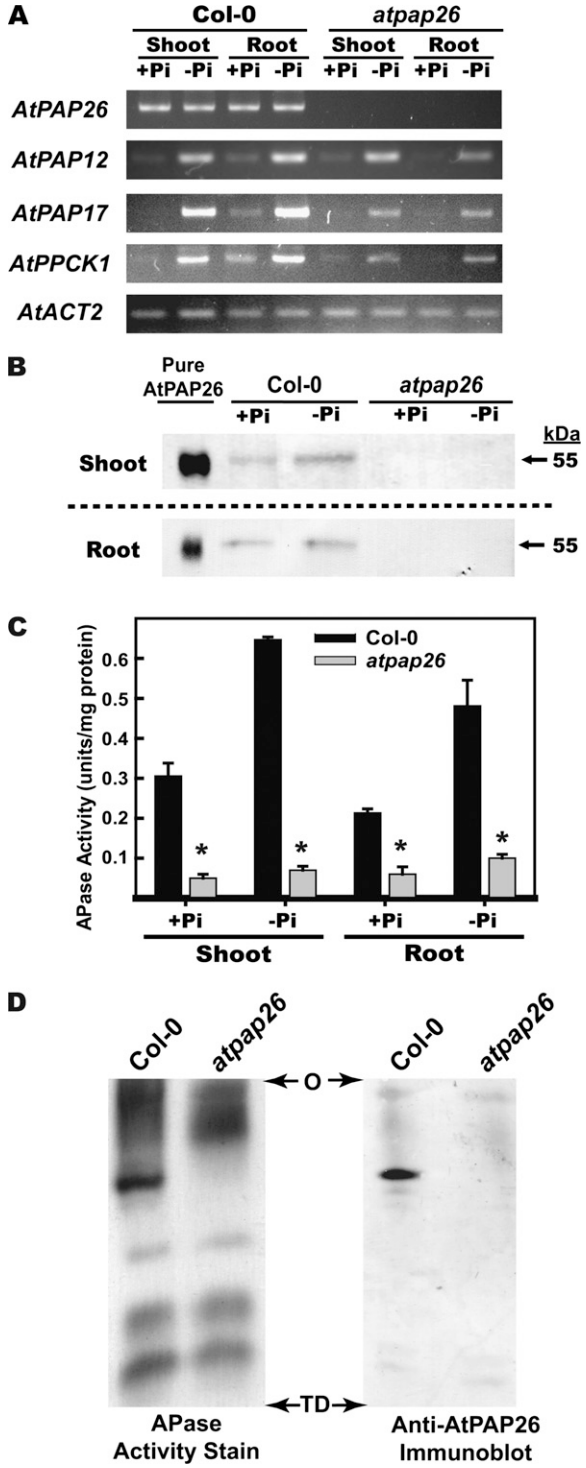


**Figure 2.** AtPAP26 is the predominant intracellular APase isozyme upregulated by −Pi Arabidopsis and whose expression is nullified in *atpap26* mutant seedlings. RNA and soluble proteins were isolated from seedlings cultivated in liquid media containing 0.2 mM Pi for 7 d prior to transfer into media containing 0 (−Pi) or 1.5 mM Pi (+Pi) for an additional 7 d. A, Levels of mRNA were analyzed by semiquantitative RT-PCR using gene-specific primers for *AtPAP12*, *AtPAP17*, *AtPAP26*, *AtPPCK1*, and *AtACT2*. *AtACT2* was used as a reference to ensure equal template loading. Control RT-PCR reactions lacking reverse transcriptase did not show any PCR product. B, Purified native AtPAP26 from −Pi Arabidopsis suspension cells (50 ng/lane; Veljanovski et al., 2006) and clarified extract proteins from shoots (2 $\mu$g/lane) and roots (4 $\mu$g/lane) of the +Pi and −Pi seedlings were resolved by SDS-PAGE and electroblotted onto a poly(vinylidene difluoride) membrane. Following oxidation of antigenic glycosyl groups with sodium-*m*-periodate (Laine, 1988), blots were probed with a 1,000-fold dilution of anti-(native AtPAP26)-immune serum and immunoreactive polypeptides detected using an alkaline-phosphatase-linked secondary antibody and chromogenic detection (Veljanovski et al., 2006). C, APase activity of clarified extracts represent means (±SE) of duplicate assays on $n = 3$ biological replicates; asterisks denote values that are significantly different from Col-0 ($P < 0.01$). D, Clarified extracts from −Pi shoots of Col-0 and *atpap26* were resolved by nondenaturing PAGE and subjected to in-gel APase activity staining (50 $\mu$g protein/lane) or immunoblotting with anti-(native AtPAP26)-immune serum (7 $\mu$g protein/lane). O, Origin; TD, tracking dye front.

strongly cross-reacted with the anti-AtPAP26 immune serum was absent in the *atpap26* mutant (Fig. 2D). Similarly, nondenaturing PAGE of concentrated secretome proteins of −Pi Col-0 seedlings revealed a prominent PSI APase activity-staining band comigrating with purified AtPAP26 that was missing in the secretome of the −Pi atpap26 mutant. Collective results of Figures 2 and 3 support earlier biochemical studies (Veljanovski et al., 2006; Tran et al., 2010b), and confirm that AtPAP26 is a principal contributor of intracellular and secreted APase activity of −Pi Arabidopsis. Similar results were obtained by Tomscha and coworkers (2004) who characterized an Arabidopsis phosphatase underproducer (*pup3*) ethylmethane sulfonate mutant that exhibited about 40% lower APase activity in shoot and root extracts. Although immunoblotting using antiserum raised against recombinant AtPAP12 led them to conclude that AtPAP12 was one of the AtPAP isozymes defective in *pup3*, AtPAP26 was also implicated since the *pup3* mutation mapped to a 2.7 Mb sequence of chromosome 5 within the Arabidopsis genome that encompasses *AtPAP26* (Tomscha et al., 2004). That *pup3* may have been defective in AtPAP26 rather than AtPAP12 is supported by the observations that: (1) *AtPAP12* transcript levels were unaffected in *pup3* (Tomscha et al., 2004), whereas (2) the same anti-recombinant AtPAP12 immune serum employed by Tomscha et al. (2004) effectively cross-reacts with both AtPAP12 and AtPAP26 (Fig. 3A; Tran et al., 2010b). By contrast, no detectable influence on total APase activity was obtained with several other AtPAP isozyme loss-of-function mutants. For example, no alteration in extractable APase activity was reported in *atpap23* T-DNA mutants (Zhu et al., 2005). Similarly, extracts of *atpap15* T-DNA mutants contained 6-fold lower phytase activity, but unaltered *p*NPP hydrolytic activity relative to wild-type controls, possibly due to AtPAP15's specificity as a phytase (Zhang et al., 2008) and/or its low abundance relative to AtPAP26.

### AtPAP26 Is Essential for Efficient Acclimation of Arabidopsis to Pi Starvation

The influence of Pi nutrition on the development of Col-0 versus *atpap26* plants was initially compared by examining their growth on +Pi and −Pi Murashige and Skoog agar media. No differences were noted in the appearance or average fresh weight of shoots of 14-d-old +Pi Col-0 versus *atpap26* seedlings (Fig. 4A; data not shown). However, *atpap26* shoot development was significantly disrupted during growth on −Pi media, exhibiting a 30% decrease in fresh weight relative to Col-0 (Fig. 4A). The development of *atpap26* mutants was also characterized in plants cultivated on +Pi or −Pi agar media, as well as on +Pi media deficient in nitrogen or potassium, or supplemented with 1 $\mu$M paraquat. Similar to 14-d-old plants (Fig. 4B), rosette fresh weight of 3-week-old −Pi *atpap26* seedlings was reduced by about 25% relative to −Pi Col-0, but unaffected under +Pi conditions (Fig. 4B). Likewise, no phenotypic differences relative to Col-0 were apparent when +Pi *atpap26* seedlings were sub-

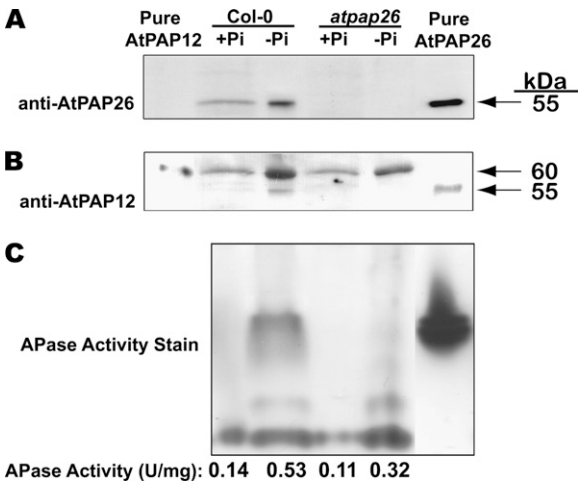


**Figure 3.** Immunological AtPAP detection, in-gel APase activity staining, and corresponding APase-specific activities of proteins secreted into the media by +Pi and −Pi Col-0 and *atpap26* seedlings. Growth medium containing secreted proteins was passed through a 0.45 $\mu$m filter and concentrated >250-fold with Amicon Ultra-15 ultrafiltration devices (30,000 $M_r$ cutoff; Millipore) at room temperature. A and B, Concentrated proteins (15 $\mu$g/lane) as well as homogeneous AtPAP12 and AtPAP26 from −Pi Arabidopsis suspension cells (Tran et al., 2010b; 20 ng each) were subjected to SDS-PAGE and immunoblotting as described in the legend for Figure 2, except that the immunoreactive polypeptides were visualized using a horseradish peroxidase-conjugated secondary antibody and enhanced chemiluminescent detection (ECL Plus, GE Healthcare). C, Concentrated secreted proteins (30 $\mu$g/lane) and homogenous AtPAP26 (1 $\mu$g; Tran et al., 2010b) were subjected to nondenaturing PAGE and in-gel APase activity staining as described in the legend for Figure 2D. APase activity was also assayed from the concentrated liquid media collected from seedlings cultivated as described in the legend for Figure 2. All APase activities represent the means of duplicate determinations on $n = 3$ biological replicates and are reproducible to within ±15% of the mean value.

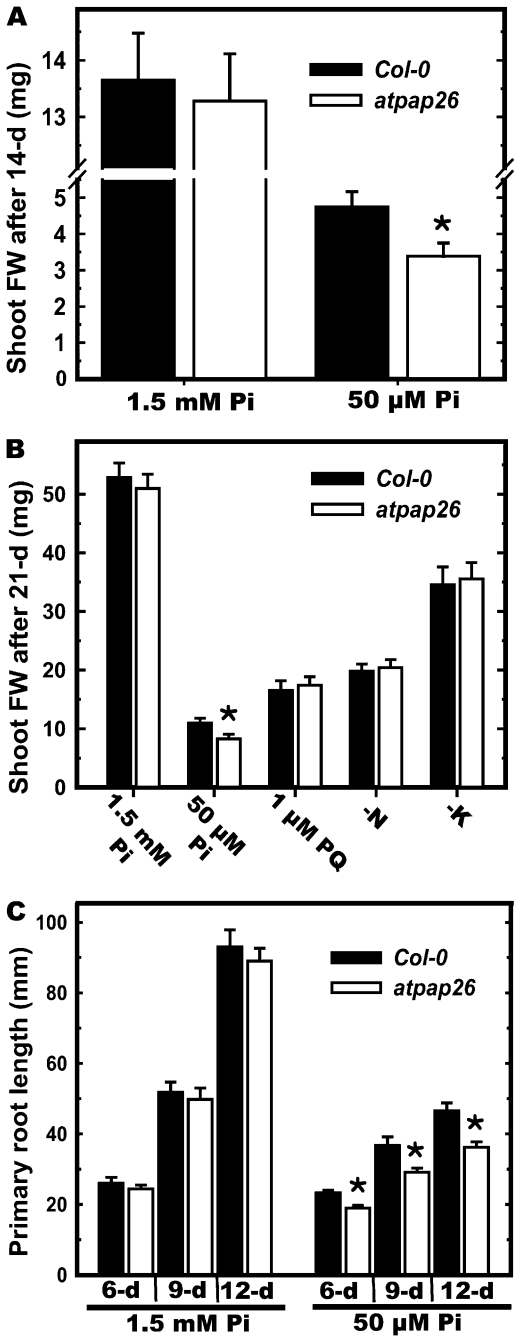


**Figure 4.** Influence of nutrient deprivation or oxidative stress on growth of *atpap26* and Col-0 seedlings. A, Shoot fresh weight (FW) of seedlings cultivated for 14 d under continuous illumination (100 $\mu$mol $m^{-2}$ $s^{-1}$ photosynthetically active radiation) on agar-solidified 0.5× Murashige and Skoog media containing 1% Suc and 1.5 mM or 50 $\mu$M Pi. B, Shoot fresh weight of seedlings cultivated on agar media containing 1.5 mM Pi for 7 d, then grown for an additional 14 d on media containing 1.5 mM or 50 $\mu$M Pi, or on +Pi media lacking nitrogen (−N) or potassium (−K), or containing 1 $\mu$M paraquat (PQ). C, Primary root length of seedlings cultivated on vertically oriented plates for 6, 9, or 12 d as described in A. All values in A to C represent means ± SE of $n = 16$ seedlings from four different plates; asterisks denote values that are significantly different from Col-0 ($P < 0.01$).

jected to nitrogen or potassium deficiency, or paraquat treatment (Fig. 4B; data not shown). Loss of AtPAP26 function also failed to influence the sensitivity of Arabidopsis to paraquat-mediated oxidative stress, suggesting that the in vitro alkaline peroxidase activity of purified AtPAP26 (Veljanovski et al., 2006) has little in vivo relevance during Pi stress. This is consistent with AtPAP26's vacuolar localization (Carter et al., 2004; and see below) in which an acidic pH of about pH 5.5 closely aligns with the enzyme's APase pH-activity optimum of pH 5.6, but is far below AtPAP26's peroxidase pH-activity optimum of pH 9.0 (Veljanovski et al., 2006). It therefore appears that while AtPAP26 is indispensable for the acclimation of Arabidopsis to Pi deprivation, it is expendable in +Pi Arabidopsis, or during other macronutrient deficiencies or oxidative stress.

Root development of the *atpap26* mutant was examined by cultivating seedlings on vertically orientated agar plates for 12 d. Decreasing the Pi concentration in the growth media resulted in a substantial reduction in primary root growth of *atpap26* and Col-0 seedlings (Fig. 4D), as well as increased root hair proliferation (Supplemental Fig. S1B). However, primary roots of the *atpap26* mutant were about 20% shorter than those of Col-0 during growth on the −Pi media (Fig. 4D; Supplemental Fig. S1A). By contrast, there was no obvious influence of the loss of *AtPAP26* expression on root structure architecture of +Pi or −Pi seedlings, or root hair number within 5 mm of the root tip (Supplemental Fig. S1).

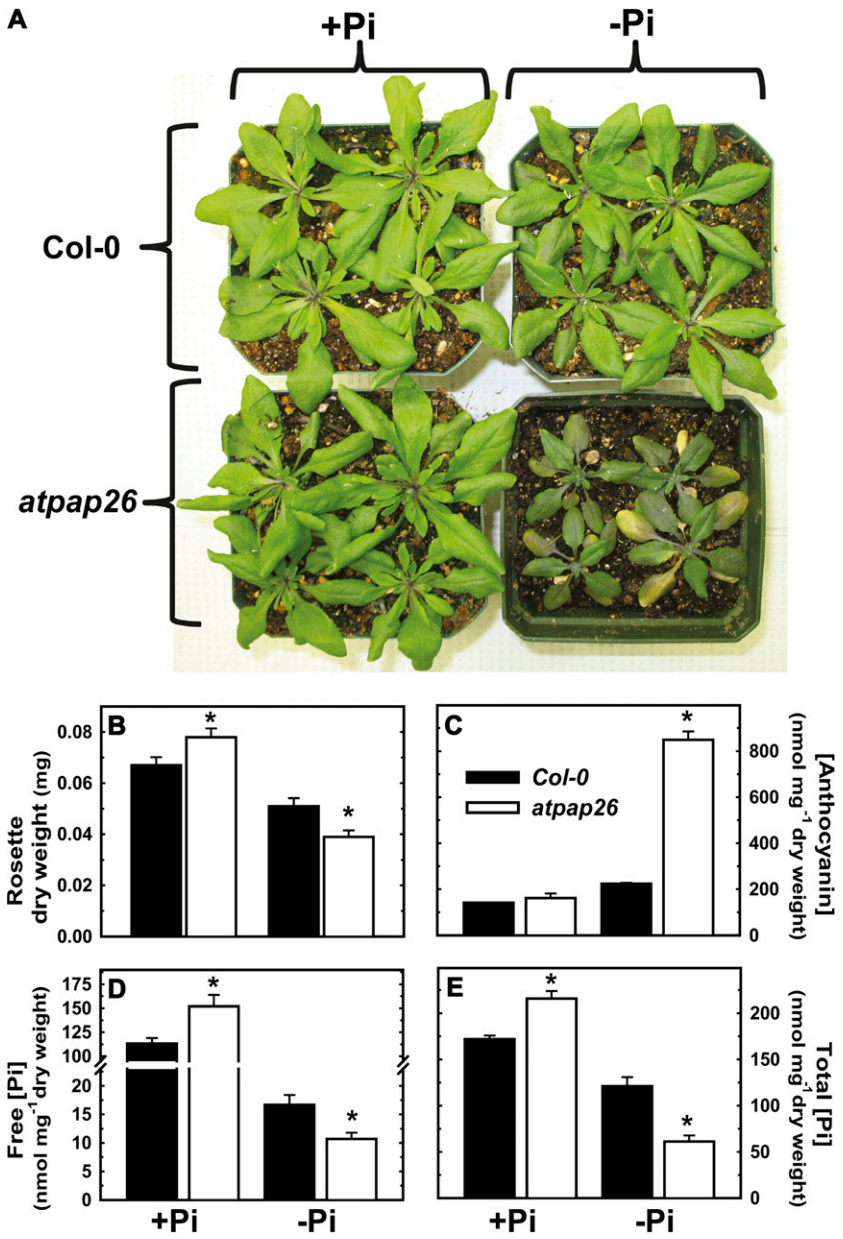


**Figure 5.** Effect of Pi deprivation on soil-grown *atpap26* and Col-0 seedlings. A, Seedlings were cultivated for 7 d on Pi-fertilized soil, then transplanted into a Pi-deficient soil mixture and grown for an additional 14 d; fertilization occurred biweekly with 0.25× Hoagland media containing 2 mM Pi (+Pi) or 0 mM Pi (−Pi). Pots shown are representative of 10 replicates. B, Rosette dry weight of seedlings cultivated as in A. C to E, Anthocyanin (C), and free and total Pi concentrations (D and E) of rosette leaves of seedlings cultivated as in A. All values are means ± SE ($n$ = 20 for B, 5 for C, and 10 for D and E); asterisks denote values that are significantly different from Col-0 ($P < 0.01$).

Although altered root development is a common phenomenon within functional analyses of Arabidopsis PSI genes, this response can be grouped into two categories based on the function of the PSI gene in question. Disruption of genes involved in transcriptional reorganization or hormone-mediated responses to Pi starvation generally causes a shift in root structure architecture in addition to decreased primary root growth. For example, knockout of PSI transcription factors has been reported to reduce primary root growth with concomitant increases in lateral root and root hair development (Devaiah et al., 2007a, 2007b). Similar results have been obtained with genes that mediate signal transduction in −Pi Arabidopsis, such as phospholipase Dζ1 and Dζ2, in which a double knockout exhibited reduced phosphatidic acid levels and altered root structure architecture during Pi starvation (Li et al., 2006). By contrast, disruption of PSI genes encoding metabolic enzymes often results in a reduction of total root growth during Pi stress without obvious changes in root structure architecture. For example, knockout of *monogalactosyldiacylglycerol synthase2* resulted in an overall 20% decrease in root growth, without influencing root structure architecture (Kobayashi et al., 2009). The observed up-regulation of three well-documented PSI genes (Fig. 2A) and overall reduced root growth without concomitant alterations in root structure architecture are consistent with AtPAP26's function in Pi scavenging and recycling, rather than Pi signaling, during Pi starvation.

PSI gene expression is influenced by sugar levels (Karthikeyan et al., 2006), while exogenous Suc may exacerbate Pi starvation through increased cell proliferation signaling (Lai et al., 2007). As plant cultivation under sterile conditions in the presence of exogenous Suc may generate phenotypes not seen under more physiologically relevant conditions we examined whether soil-grown *atpap26* plants displayed any phenotype. The *atpap26* mutant exhibited markedly impaired development during cultivation for 14 d under −Pi conditions on a nutrient-depleted soil mixture (Fig. 5A), as reflected by the 25% reduction in rosette dry weight relative to Col-0 control plants (Fig. 5B). By contrast, *atpap26* plants showed a small, but significant 16% increase in rosette dry weight during their cultivation on +Pi soil. Similar to seedlings cultivated in sterile liquid media (Fig. 2C), the extractable APase activity of soil-grown *atpap26* mutant plants was much lower than that of Col-0 controls. Clarified extracts prepared from fully expanded leaves of 3-week-old −Pi *atpap26* plants exhibited about 4- and 11-fold lower PEP- and *p*NPP-hydrolyzing activity, respectively, relative to Col-0 (60 ± 6 and 212 ± 37 nmol PEP versus 36 ± 4 and 530 ± 44 nmol *p*NPP hydrolyzed $min^{-1}$ $mg^{-1}$ protein, respectively; means ± SE of $n = 4$ biological replicates).

One of the most obvious symptoms of plant Pi stress is anthocyanin accumulation in shoots that is believed to protect chloroplasts against photoinhibition (Vance et al., 2003). Since petioles of soil-cultivated −Pi *atpap26* plants were purple in color (Fig. 5A) their leaf anthocyanin content was quantified. Although anthocyanins accumulated in Col-0 and *atpap26* leaves during growth on the −Pi soil, the anthocyanin level of *atpap26* leaves was about 5-fold greater than that of Col-0 (Fig. 5C). The stunted development of −Pi *atpap26* seedlings coupled with their drastically elevated shoot anthocyanin levels suggested that the mutant was suffering from more pronounced nutritional Pi deficiency relative to Col-0. Indeed, a 35% and 50% reduction in free and total Pi concentration, respectively, was quantified in leaves of −Pi *atpap26* plants, relative to Col-0 controls (Fig. 5D). This adds further support for AtPAP26's critical role in the Pi metabolism of −Pi Arabidopsis. The peat-vermiculite soil mix used in these experiments contained 12.8 ± 0.5 μmol total Pi $g^{-1}$ dry weight (mean ± SE, of $n = 3$ determinations). However, all Pi present in this soil was in the form of organic P, as its free Pi content was undetectable. Since AtPAP26 is also secreted by Arabidopsis roots during Pi stress (Fig. 3; Tran and Plaxton, 2008; Tran et al., 2010b) it is possible that decreased hydrolysis of soil-localized organic P reduced the total amount of Pi made available to the *atpap26* mutant

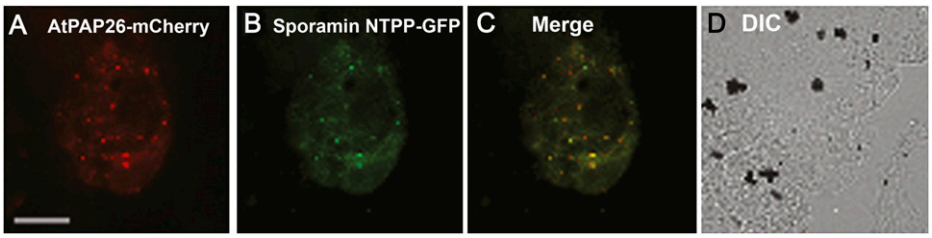


**Figure 6.** AtPAP26-mCherry localizes to lytic vacuoles of transiently transformed Arabidopsis suspension cells. Heterotrophic suspension cells were transiently cotransformed via biolistic bombardment with AtPAP26-mCherry and sporamin NTPP-GFP. Following bombardment, cells were incubated for 8 h to allow for gene expression and protein sorting, then fixed in formaldehyde and viewed using epifluorescence microscopy. Note that the fluorescence patterns attributable to coexpressed AtPAP26-mCherry (A) and sporamin NTPP-GFP (B) colocalize in the same cell, as evidenced by yellow color in the merged image (C). Also shown (D), is the differential interference contrast (DIC) image of the cell depicted in A to C. This result is representative of ≥25 cells from at least two independent biolistic bombardments. Bar = 10 μm.

during its cultivation on the Pi-deficient soil. In contrast to −Pi conditions, the *atpap26* leaves accumulated about 25% more free and total Pi relative to Col-0 during their growth on Pi-fertilized soil (Fig. 5D). This provides a feasible basis for the small increase in rosette dry weight of soil-cultivated +Pi *atpap26* plants (Fig.5B), and indicates that AtPAP26 may also function in intracellular Pi homeostasis of +Pi plants.

### Vacuolar Localization of AtPAP26-mCherry

To determine the subcellular localization of AtPAP26, its coding region was fused with the 5′ end of a *mCherry* reporter gene and transiently expressed via biolistic bombardment in Arabidopsis suspension cells under the control of the cauliflower mosaic virus 35S promoter. Epifluorescence microscopy demonstrated that AtPAP26-mCherry was targeted to lytic vacuoles (Fig. 6A) as evidenced by its colocalization with coexpressed sporamin N-terminal propeptide (NTPP)-GFP (Fig. 6, B and C), serving as a well-characterized lytic vacuole marker fusion protein (Jin et al., 2001; Kim et al., 2001). These results are consistent with those of Carter and coworkers (2004) who reported that the protein encoded by gene locus At5g34850 (i.e. AtPAP26) is a member of the vacuolar proteome of Arabidopsis leaves.

## CONCLUSION

Results of this study corroborate parallel biochemical analyses, indicating that *AtPAP26* encodes the principal vacuolar, as well as a major secreted APase isozyme up-regulated by −Pi Arabidopsis (Veljanovski et al., 2006; Tran and Plaxton, 2008; Tran et al., 2010b). However, in contrast to PSI enzymes such as AtPAP12 and AtPAP17, AtPAP26's enhanced synthesis during Pi deprivation is under posttranscriptional control (Fig. 3). Recent proteomic studies established that transcriptional controls exert little influence on levels of certain intracellular and secreted proteins up-regulated by −Pi plants relative to translational and posttranslational controls that influence protein synthesis and degradation (see Tran and Plaxton 2008 and refs. therein). This highlights the need to integrate transcriptomics with parallel biochemical and proteomic analyses of plant stress responses, as the combined datasets will provide a far better depiction of how alterations in gene expression may be linked to adaptive changes in plant metabolism. As the predominant APase isozyme up-regulated by −Pi Arabidopsis, it was not unexpected that the development of *atpap26* seedlings was specifically disrupted during their cultivation on −Pi media (Figs. 4 and 5). Shoots of soil-grown *atpap26* mutants accumulated significantly less free and total Pi relative to Col-0 during Pi stress (Fig. 5). This supports the hypothesis that AtPAP26 functions to recycle and scavenge Pi from intracellular and extracellular P-ester pools, respectively, so as to enhance the overall Pi utilization efficiency of −Pi Arabidopsis. Eliminating the expression of genes encoding PSI metabolic enzymes has been reported to disrupt the growth of −Pi Arabidopsis, albeit in the context of altered Pi recycling from membrane phospholipids due to loss of the PSI phospholipase-C isoform NPC5, or monogalactosyldiacylglycerol synthase2 (Gaude et al., 2008; Kobayashi et al., 2009). Similarly, loss of PSI high-affinity Pi transporters disrupted the shoot development of −Pi, but not +Pi Arabidopsis (Shin et al., 2004). However, to our knowledge, this is the first study showing that elimination of a single member of the AtPAP family simultaneously exerts a significant inhibitory effect on nonspecific APase activity and growth of −Pi Arabidopsis.

Several studies have reported that overexpression of secreted PAPs can improve plant biomass and Pi accumulation (Xiao et al., 2006; Hur et al., 2007; Ma et al., 2009; Wang et al., 2009). However, these attempts have either focused around high-specificity phytases or PAPs with extracellular roles, but unclear intracellular function. On the other hand, AtPAP26 not only has a demonstrated vacuolar localization (Fig. 6; Veljanovski et al., 2006), but is a dual-targeted enzyme that is also secreted by −Pi Arabidopsis (Fig. 3; Tran and Plaxton, 2008; Tran et al., 2010b). Although differential glycosylation appears to be involved in AtPAP26's dual targeting to the vacuole versus extracellular space of −Pi Arabidopsis, the precise molecular and cellular mechanisms underlying this phenomenon remain to be investigated. Intracellular and secreted AtPAP26 glycoforms of −Pi Arabidopsis are highly active against a wide range of P-ester substrates over a broad pH range (Veljanovski et al., 2006; Tran et al., 2010b), making AtPAP26 a promising candidate for biotechnological strategies aimed at improving crop Pi acquisition and utilization. It will thus be of interest to examine the Pi metabolism and growth characteristics of *AtPAP26* overexpressors cultivated on unfertilized soil and/or with various P-esters as their sole source of exogenous P.

## MATERIALS AND METHODS

### Plant Material and Growth Conditions

For mutant isolation and routine plant growth Arabidopsis (*Arabidopsis thaliana*; Col-0 ecotype) seeds were sown in a standard soil mixture (Sunshine Aggregate Plus Mix 4; SunGro) and stratified at 4°C for 2 d. Plants were cultivated in growth chambers at 22°C (16/8 h photoperiod at 100 $\mu$mol $m^{-2}$ $s^{-1}$), and fertilized biweekly by subirrigation with 0.25× Hoagland media. To assess the influence of Pi deprivation on the development of soil-grown plants, 7-d-old seedlings were transplanted into a 75% to 85% sphagnum peat moss/perlite soil mix lacking all nutrients (Sunshine Mix 2; SunGro) at a density of four seedlings per pot. Plants were fertilized biweekly with 0.25× Hoagland media containing either 2 or 0 mM Pi. At 3 weeks post germination entire rosettes were harvested and either dried for 48 h at 65°C, or snap frozen in liquid $N_2$, and stored at −80°C for later analysis. Whenever Pi was reduced or eliminated from the growth medium, Pi salts were replaced with appropriate sulfate salts, so that the conjugate cation remained constant.

For liquid culture, approximately 100 seeds were surface sterilized and stratified for 2 d at 4°C, then placed in 250 mL magenta boxes containing 50 mL of 0.5× Murashige and Skoog media, pH 5.7, 1% (w/v) Suc, and 0.2 mM Pi, and cultivated at 24°C under continuous illumination (100 $\mu$mol $m^{-2}$ $s^{-1}$) on an orbital shaker set at 80 rpm. After 7 d the seedlings were transferred into fresh media containing 1.5 or 0 mM Pi for an additional 7 d. The 14-d-old seedlings were blotted dry, snap frozen in liquid $N_2$, and stored at −80°C, whereas growth media containing secreted proteins was passed through a 0.45 $\mu$m filter and concentrated over 250-fold with an Amicon Ultra-15 ultrafiltration device (30,000 $M_r$ cutoff; Millipore) at room temperature (23°C).

## Mutant Isolation

A potential *atpap26* (Salk_152821) mutant line was identified from the Salk T-DNA lines (Alonso et al., 2003) via analyses of the SiGnAL database (http://signal.salk.edu/cgi-bin/tdnaexpress). Seeds were obtained from the Arabidopsis Biological Resource Center (ABRC) at Ohio State University. Homozygous mutant plants were isolated by PCR screening of gDNA from the T4 generation using primers mapped on Figure 1A and described in Supplemental Table S1. All PCR products were sequenced for verification (Génome Québec). Southern blotting was performed on *atpap26* gDNA to determine T-DNA insert number. gDNA was isolated according to Zhang and Zeevaart (1999) except that isopropanol-precipitated nucleic acids were pelleted by centrifugation at 15,000*g* for 10 min, followed by two washes with 70% (v/v) ethanol; DNA pellets were dissolved in 10 mM Tris-HCl (pH 8.0). Gel-blot analysis was performed as described (Quan et al., 2007). The 795 bp neomycin phosphotransferase coding sequence (*NPTII* CDS) was used to generate a digoxigenin (dig)-labeled probe using Roche's dig labeling kit. Southern-blot hybridization was performed at 70°C for 18 h using hybridization solution (250 mM NaPi, pH 7.2, 1 mM EDTA, 20% [w/v] SDS, 0.5% [w/v] milk powder) with dig-labeled *NPTII* CDS probes followed by three 20 min washes at 60°C in 20 mM NaPi (pH 7.2) containing 1 mM EDTA and 1% (w/v) SDS. The blot was incubated for 90 min in 1% (w/v) milk powder and probed for 30 min with 1:5,000 anti-dig-IgG conjugated to alkaline phosphatase (Roche), followed by two 15 min washes in detection wash solution. Bands were visualized by chemiluminescence using CDP-Star (Roche).

## RNA Isolation and Semiquantitative RT-PCR

Total RNA was extracted and purified as described previously (Veljanovski et al., 2006). RNA samples were assessed for purity via their $A_{260}/A_{280}$ ratio and integrity by resolving 1 $\mu$g of total RNA on a 1.2% (w/v) denaturing agarose gel. Normalization of RNA for RT was performed for each sample by density measurement of 28S ribosomal RNA bands from the above gel (scanned using ImageJ software from the National Institutes for Health). RNA (5 $\mu$g) was reverse transcribed with Superscript III (Invitrogen) and noncompetitive RT-PCR was performed as described in Gennidakis et al. (2007). Primers used to amplify *AtPPCK1*, *AtPAP17*, *AtPAP26*, and *AtACT2* were previously described (Veljanovski et al., 2006; Gregory et al., 2009). Transcripts for *AtPAP12* were amplified using gene-specific primers (Supplemental Table S1); all PCR products were sequenced for verification. Conditions were optimized for all semiquantitative RT-PCR reactions to ensure linearity of response for comparison between samples.

## Protein Extraction, APase Assays, and Determination of Protein Concentration

Tissues were homogenized (1:2; w/v) in ice-cold extraction buffer composed of 20 mM sodium acetate (pH 5.6), 1 mM EDTA, 1 mM dithiothreitol, 1 mM phenylmethlysulfonyl fluoride, 5 mM thiourea, and 1% (w/v) insoluble polyvinyl (polypyrrolidone). Homogenates were centrifuged at 4°C and 14,000*g* for 5 min, and the supernatants reserved as clarified extract. APase activity was routinely measured at 25°C by coupling the hydrolysis of PEP to pyruvate to the lactate dehydrogenase reaction and continuously monitoring NADH oxidation at 340 nm using a Molecular Devices Spectromax Plus microplate spectrophotometer and the following optimized assay conditions: 50 mM Na acetate (pH 5.6), 5 mM PEP, 10 mM $MgCl_2$, 0.2 mM NADH, and 3 units of rabbit muscle lactate dehydrogenase in a final volume of 0.2 mL. Assays were corrected for background NADH oxidation by omitting PEP from the reaction mixture. APase assays were also carried out in an assay mix containing 50 mM sodium acetate (pH 5.6), 5 mM *p*NPP, and 10 mM $MgCl_2$ by monitoring the formation of *para*-nitrophenol at 405 nm ($\varepsilon$ = 18.2 $mM^{-1}$ $cm^{-1}$). All APase assays were linear with respect to time and concentration of enzyme assayed. One unit of activity is defined as the amount of enzyme resulting in the hydrolysis of 1 $\mu$mol of substrate $min^{-1}$ at 25°C. Protein concentrations were determined using a modified Bradford assay (Bozzo et al., 2002) with bovine $\gamma$-globulin as the standard.

## Protein Electrophoresis and Immunoblotting

SDS-PAGE, immunoblotting onto poly(vinylidene difluoride) membranes (Immobilon transfer; 0.45 $\mu$m pore size; Millipore Canada), and visualization of antigenic polypeptides using an alkaline-phosphatase-tagged secondary antibody were conducted as previously described (Veljanovski et al., 2006; Tran and Plaxton, 2008). Densitometric analysis of immunoblots was performed using an LKB Ultroscan XL laser densitometer and GELSCAN software (version 2.1; Pharmacia LKB Biotech). Derived $A_{660}$ values were linear with respect to the amount of the immunoblotted extract. All immunoblot results were replicated a minimum of three times, with representative results shown in the various figures. Nondenaturing PAGE was carried out using 7% separating gels (Gennidakis et al., 2007). In-gel APase activity staining was performed by equilibrating the gels in 100 mM Na acetate (pH 5.6) containing 10 mM $MgCl_2$ for 30 min, and then incubating in equilibration buffer containing 1 mg $mL^{-1}$ Fast Garnet GBC and 0.03% (w/v) $\beta$-naphthyl-*P*.

## Quantification of Total and Soluble Pi

Total Pi determinations were carried out using dried leaf tissue that had been flamed to ash by heating at 500°C for 3 h. The ash was dissolved in 30% (v/v) HCl containing 10% (v/v) $HNO_3$, and centrifuged at 14,000*g* for 10 min. The supernatant was diluted 50-fold in water and its Pi concentration quantified as previously described (Bozzo et al., 2006). Diluted sample (800 $\mu$L) was mixed with 200 $\mu$L of a Pi assay reagent and incubated at 45°C for 20 min. Pi assay reagent consisted of four parts of freshly prepared 10% (w/v) ascorbic acid plus one part 10 mM ammonium molybdate containing 15 mM zinc acetate (pH 5.0). Total Pi content was measured at $A_{660}$ using appropriate Pi standards and is expressed as $\mu$mol Pi $mg^{-1}$ dry weight. Soluble Pi was determined by extracting frozen tissues (1:5; w/v) with 1% glacial acetic acid. Samples were centrifuged at 14,000*g* and supernatants assayed for Pi as described above. For available soil Pi, 0.5 g of soil was suspended in 10 mL of deionized water and the eluate removed for free Pi determination. To determine the total amount of Pi in the soil, 1 g was converted to ash as described above prior to Pi determination.

## Determination of Anthocyanin Concentration

Frozen leaf material was transferred to extraction buffer (18% [v/v] 1-propanol containing 1% [v/v] concentrated HCl), and then the extraction vials were placed in a boiling water bath for 3 min. Extracts were centrifuged at 14,000*g* for 10 min and the absorbance was measured at 532 and 653 nm. Subtraction of $0.24A_{653}$ compensated for the small overlap in $A_{532}$ by the chlorophylls (Schmidt and Mohr, 1981). Anthocyanin concentration was determined using the corrected absorbance ($\varepsilon$ = 38,000 $M^{-1}cm^{-1}$).

## Subcellular Localization of AtPAP26-mCherry Fusion Protein

An *AtPAP26* cDNA clone (U11049) was obtained from ABRC, and amplified using PCR and appropriate oligonucleotide primers (Supplemental Table S1). The resulting PCR fragment, containing the entire open reading frame of *AtPAP26*, was inserted into *Eco*RI to *Xma*I of plasmid *pSAT4A-mCherry-N1* (ABRC) to yield *pSAT4A-AtPAP26-mCherry*. The plasmid, *p35S-NTPP-GFP*, encoding the Arabidopsis basic chitinase N-terminal signal sequence, followed by the 16-amino-acid long sweet potato (*Ipomoea batatas*) sporamin NTPP fused to the GFP was a gift from Christopher Trobacher and John Greenwood (University of Guelph, Canada) and was constructed in the following manner. First, the plasmid *p35S-mGFP5-HDEL* (provided by Jim Haseloff, University of Cambridge, United Kingdom) containing the 35S cauliflower mosaic virus promoter driving the expression of a fusion protein consisting of the Arabidopsis basic chitinase signal sequence fused to GFP and a C-terminal HDEL endoplasmic reticulum retrieval sequence (Haseloff et al., 1997) was modified (using the Quikchange PCR-based site-directed muta-

genesis kit [Stratagene] and appropriate oligonucleotide primers; Supplemental Table S1) to introduce an *Xho*I site following the basic chitinase signal sequence. Thereafter, *p35S-mGFP5-HDEL* was modified further (via site-directed mutagenesis) to replace the codon encoding the histidine at the −4 position of the −HDEL endoplasmic reticulum retrieval motif with a stop codon, yielding *p35S-mGFP5-NXS*. Finally, annealed (complementary) oligonucleotides encoding the 16-amino-acid long sporamin NTPP containing lytic vacuolar sorting information (Matsuoka and Nakamura, 1991; Koide et al., 1997), along with *Xho*I compatible ends, were ligated directly into *Xho*I-digested *p35S-mGFP5-NXS*, yielding *p35S-NTPP-GFP*.

Culturing of Arabidopsis (var. Landsberg *erecta*) suspension cells in standard Murashige and Skoog media (containing 1.25 mM Pi), and cotransient transformations of cells (4 d post subculturing) with 10 $\mu$g of each plasmid using a biolistic particle delivery system 1000/HE (Bio-Rad) were performed as previously described (Lingard et al., 2008). Bombarded cells were incubated for 8 h to permit expression and sorting of the expressed proteins, and then fixed in formaldehyde. Images were acquired using a Zeiss Axioscope 2 MOT epifluorescence microscope (Carl Zeiss Inc.) with a Zeiss 63× plan apochromat oil-immersion objective. Image capture was performed using a Retiga 1300 charge-coupled device camera (Qimaging) and Northern Eclipse 5.0 software (Empix Imaging Inc.). Figure compositions were generated using Adobe Photoshop CS (Adobe Systems Inc.).

## Statistics

All values are presented as means ± SE. Data were analyzed using the one-tailed Student's *t* test, and deemed significant if $P < 0.01$.

## Supplemental Data

The following materials are available in the online version of this article.

**Supplemental Figure S1.** Influence of Pi deprivation on root development of 12-d-old Col-0 and *atpap26* mutant seedlings.

**Supplemental Table S1.** Primers used for cloning and RT-PCR analysis.

## ACKNOWLEDGMENTS

We thank Professor Thomas McKnight (Texas A&M University) for providing the anti-AtPAP12 immune serum, Professors Christopher Trobacher and John Greenwood (University of Guelph) for the *p35S-NTPP-GFP* plasmid, and Professor Jim Haseloff (University of Cambridge) for the *p35S-mGFP5-HDEL* plasmid. We are also grateful to the Analytical Services Unit of Queen's University for providing access to their 500°C oven.

Received January 11, 2010; accepted March 23, 2010; published March 26, 2010.

## LITERATURE CITED

**Alonso JM, Stepanova A, Leisse TJ, Kim CJ, Chen H, Shinn P, Stevenson DK, Zimmerman J, Barajas P, Cheuk R, et al** (2003) Genome-wide insertional mutagenesis of *Arabidopsis thaliana*. Science **301:** 653–657

**Bozzo GG, Dunn EL, Plaxton WC** (2006) Differential synthesis of phosphate-starvation inducible purple acid phosphatase isozymes in tomato (*Lycopersicon esculentum*) suspension cells and seedlings. Plant Cell Environ **29:** 303–313

**Bozzo GG, Plaxton WC** (2008) The role of intracellular and secreted purple acid phosphatases in tomato phosphate nutrition. *In* V Preddy, R Watson, eds, Tomatoes and Tomato Products. Science Publishers, Enfield, NH, pp 216–233

**Bozzo GG, Raghothama KG, Plaxton WC** (2002) Purification and characterization of two secreted purple acid phosphatase isozymes from phosphate-starved tomato (*Lycopersicon esculentum*) cell cultures. Eur J Biochem **269:** 6278–6286

**Bozzo GG, Raghothama KG, Plaxton WC** (2004a) Structural and kinetic properties of a novel purple acid phosphatase from phosphate-starved tomato (*Lycopersicon esculentum*) cell cultures. Biochem J **377:** 419–428

**Bozzo GG, Singh VK, Plaxton WC** (2004b) Phosphate or phosphite addition promotes the proteolytic turnover of phosphate-starvation inducible tomato purple acid phosphatase isozymes. FEBS Lett **573:** 51–54

**Carter C, Pan S, Zouhar J, Avila EL, Girke T, Raikhel NV** (2004) The vegetative vacuole proteome of *Arabidopsis thaliana* reveals predicted and unexpected proteins. Plant Cell **16:** 3285–3303

**del Pozo JC, Allona I, Rubio V, Leyva A, de la Pena A, Aragoncillo C, Paz-Ares J** (1999) A type 5 acid phosphatase gene from *Arabidopsis thaliana* is induced by phosphate starvation and by some other types of phosphate mobilizing/oxidative stress conditions. Plant J **19:** 579–589

**Devaiah BN, Karthikeyan AS, Raghothama KG** (2007a) WRKY75 transcription factor is a modulator of phosphate acquisition and root development in *Arabidopsis*. Plant Physiol **143:** 1789–1801

**Devaiah BN, Nagarajan VK, Raghothama KG** (2007b) Phosphate homeostasis and root development in Arabidopsis are synchronized by the zinc finger transcription factor ZAT6. Plant Physiol **145:** 147–159

**Francisca Li WY, Shao G, Lam H** (2008) Ectopic expression of *GmPAP3* alleviates oxidative damage caused by salinity and osmotic stresses. New Phytol **178:** 80–91

**Fukuda T, Saito A, Wasaki J, Shinano T, Osaki M** (2007) Metabolic alterations proposed by proteome in rice roots grown under low P and high Al concentration under low pH. Plant Sci **172:** 1157–1165

**Gaude N, Nakamura Y, Scheible W, Ohta H, Dörmann P** (2008) Phospholipase C5 (NPC5) is involved in galactolipid accumulation during phosphate limitation in leaves of *Arabidopsis*. Plant J **56:** 28–39

**Gennidakis S, Rao SK, Greenham K, Uhrig RG, O'Leary BM, Snedden WA, Lu C, Plaxton WC** (2007) Bacterial- and plant-type phospho*enol*-pyruvate carboxylase polypeptides interact in the hetero-oligomeric class-2 PEPC complex of developing castor oil seeds. Plant J **52:** 839–849

**Gregory AL, Hurley BA, Tran HT, Valentine AJ, She YM, Knowles VL, Plaxton WC** (2009) *In vivo* regulatory phosphorylation of the phosphoenolpyruvate carboxylase AtPPC1 in phosphate starved *Arabidopsis thaliana*. Biochem J **420:** 57–65

**Haran S, Logendra S, Seskar M, Bratanova M, Raskin I** (2000) Characterization of Arabidopsis acid phosphatase promoter and regulation of acid phosphatase expression. Plant Physiol **124:** 615–626

**Haseloff J, Siemering KR, Prasher DC, Hodge S** (1997) Removal of a cryptic intron and subcellular localization of green fluorescent protein are required to mark transgenic Arabidopsis plants brightly. Proc Natl Acad Sci USA **94:** 2122–2127

**Hur YJ, Lee HG, Jeon EJ, Lee YY, Nam MH, Yi G, Eun MY, Nam J, Lee JH, Kim DH** (2007) A phosphate starvation-induced acid phosphatase from *Oryza sativa*: phosphate regulation and transgenic expression. Biotechnol Lett **29:** 829–835

**Jin JB, Kim YA, Kim SJ, Lee SH, Kim DH, Cheong GW, Hwang I** (2001) A new dynamin-like protein, ADL6, is involved in trafficking from the trans-Golgi network to the central vacuole in *Arabidopsis*. Plant Cell **13:** 1511–1525

**Karthikeyan AS, Varadarajan DK, Jain A, Held MA, Carpita NC, Raghothama KG** (2006) Phosphate starvation responses are mediated by sugar signalling in *Arabidopsis*. Planta **225:** 907–918

**Kim DH, Eu YJ, Yoo CM, Kim YW, Pih KT, Jin JB, Kim SJ, Stenmark H, Hwang I** (2001) Trafficking of phosphatidylinositol 3-phosphate from the trans-Golgi network to the lumen of the central vacuole in plant cells. Plant Cell **13:** 287–301

**Kobayashi K, Awai K, Nakamura M, Nagatani A, Masuda T, Ohta H** (2009) Type-B monogalactosyldiacylglycerol synthases are involved in phosphate starvation-induced lipid remodelling and are crucial for low-phosphate adaptation. Plant J **57:** 322–331

**Koide Y, Hirano H, Matsuoka K, Nakamura K** (1997) The N-terminal propeptide of the precursor to sporamin acts as a vacuole-targeting signal even at the C terminus of the mature part in tobacco cells. Plant Physiol **114:** 863–870

**Lai F, Thacker J, Li Y, Doerner P** (2007) Cell division activity determines the magnitude of phosphate starvation responses in *Arabidopsis*. Plant J **50:** 545–556

**Laine AC** (1988) Significant immunological cross-reactivity of plant glycoproteins. Electrophoresis **9:** 841–844

**Li D, Zhu H, Liu K, Liu X, Leggewie G, Udvardi M, Wang D** (2002) Purple acid phosphatases of *Arabidopsis thaliana*: comparative analysis and differential regulation by phosphate deprivation. J Biol Chem **277:** 27772–27781

**Li K, Xu C, Li Z, Zhang K, Yang A, Zhang J** (2008) Comparative proteome analyses of phosphorus responses in maize (*Zea mays* L.) roots of wild-

type and a low-P-tolerant mutant reveal root characteristics associated with phosphorus efficiency. Plant J **55:** 927–939

**Li M, Qin C, Welti R, Wang X** (2006) Double knockouts of phospholipases Dζ1 and Dζ2 in *Arabidopsis* affect root elongation during phosphate-limited growth but do not affect root hair patterning. Physiol Plant **140:** 761–770

**Lingard MJ, Gidda SK, Bingham S, Rothstein SJ, Mullen RT, Trelease RN** (2008) Arabidopsis PEROXIN11c-e, FISSION1b, and DYNAMIN-RELATED PROTEIN3A cooperate in cell cycle-associated replication of peroxisomes. Plant Cell **20:** 1567–1585

**Ma XF, Wright E, Ge Y, Bell J, Xi Y, Bouton JH, Wang ZY** (2009) Improving phosphorus acquisition of white clover (*Trifolium repens* L.) by transgenic expression of plant-derived phytase and acid phosphatase genes. Plant Sci **176:** 479–488

**Matsuoka K, Nakamura K** (1991) Propeptide of a precursor to a plant vacuolar protein required for vacuolar targeting. Proc Natl Acad Sci USA **88:** 834–838

**Miller SS, Liu J, Allan DL, Menzhuber CJ, Fedorova M, Vance CP** (2001) Molecular control of acid phosphatase secretion into the rhizosphere of proteoid roots from phosphorus-stressed white lupin. Plant Physiol **127:** 594–606

**Misson J, Raghothama KG, Jain A, Jouhet J, Block MA, Bligny R, Ortet P, Creff A, Somerville S, Doumas P, et al.** (2005) A genome-wide transcriptional analysis using *Arabidopsis thaliana* Affymetrix gene chips determined plant responses to phosphate deprivation. Proc Natl Acad Sci USA **102:** 11934–11939

**Müller R, Nilsson L, Krintel C, Nielsen TH** (2004) Gene expression during recovery from phosphate starvation in roots and shoots of *Arabidopsis thaliana*. Physiol Plant **122:** 233–243

**Quan R, Lin HM, Mendoza I, Zhang Y, Cao W, Yang Y, Shang M, Chen S, Pardo JM, Guo Y** (2007) SCABP8/CBL10, a putative calcium sensor, interacts with the protein kinase SOS2 to protect *Arabidopsis* shoots from salt stress. Plant Cell **19:** 1415–1431

**Rubio V, Linhares F, Solano R, Martin AC, Iglesias J, Leyva A, Paz-Ares J** (2001) A conserved MYB transcription factor involved in phosphate starvation signaling both in vascular plants and in unicellular algae. Genes Dev **15:** 2122–2133

**Schmidt R, Mohr H** (1981) Time-dependent changes in the responsiveness to light of phytochrome-mediated anthocyanin synthesis. Plant Cell Environ **4:** 433–437

**Shin H, Shin HS, Dewbre GR, Harrison MJ** (2004) Phosphate transport in *Arabidopsis*: Pht1;1 and Pht1;4 play a major role in phosphate acquisition from both low- and high-phosphate environments. Plant J **39:** 629–642

**Tomscha JL, Trull MC, Deikman J, Lynch JP, Guiltinan MJ** (2004) Phosphatase under-producer mutants have altered phosphorus relations. Plant Physiol **135:** 334–345

**Tran HT, Hurley BA, Plaxton WC** (2010a) Feeding hungry plants: the role of purple acid phosphatases in phosphate nutrition. Plant Sci **179:** 14–27

**Tran HT, Plaxton WC** (2008) Proteomic analysis of alterations in the secretome of *Arabidopsis thaliana* suspension cells subjected to nutritional phosphate deficiency. Proteomics **8:** 4317–4326

**Tran HT, Qian W, Hurley BA, She Y, Wang D, Plaxton WC** (2010b) Biochemical and molecular characterization of AtPAP12 and AtPAP26: the predominant purple acid phosphatase isozymes secreted by phosphate-starved *Arabidopsis thaliana*. Plant Cell Environ (in press)

**Vance CP, Uhde-Stone C, Allan DL** (2003) Phosphorus acquisition and use: critical adaptations by plants for securing a nonrenewable resource. New Phytol **157:** 423–447

**Veljanovski V, Vanderbeld B, Knowles VL, Snedden WA, Plaxton WC** (2006) Biochemical and molecular characterization of AtPAP26, a vacuolar purple acid phosphatase up-regulated in phosphate-deprived Arabidopsis suspension cells and seedlings. Plant Physiol **142:** 1282–1293

**Wang X, Wang Y, Tian J, Lim BL, Yan X, Liao H** (2009) Overexpressing AtPAP15 enhances phosphorus efficiency in soybean. Plant Physiol **151:** 233–240

**Wu P, Ma L, Hou X, Wang M, Wu Y, Liu F, Deng X** (2003) Phosphate starvation triggers distinct alterations of genome expression in Arabidopsis roots and leaves. Plant Physiol **132:** 1260–1271

**Xiao K, Katagi H, Harrison M, Wang ZY** (2006) Improved phosphorus acquisition and biomass production in *Arabidopsis* by transgenic expression of a purple acid phosphatase gene for *M. trunculata*. Plant Sci **170:** 191–202

**Zakhleniuk OV, Raines CA, Lloyd JC** (2001) *pho3*: a phosphorus-deficient mutant of *Arabidopsis thaliana* (L.) Heynh. Planta **212:** 529–534

**Zhang HX, Zeevaart JAD** (1999) An efficient *Agrobacterium tumefaciens* mediated transformation and regeneration system for cotyledons of spinach (*Spinacia oleracea* L.). Plant Cell Rep **18:** 640–645

**Zhang W, Gruszewski HA, Chevone BI, Nessler CL** (2008) An Arabidopsis purple acid phosphatase with phytase activity increases foliar ascorbate. Plant Physiol **146:** 431–440

**Zhu H, Qian W, Xuzhong L, Li D, Liu X, Liu K, Wang D** (2005) Expression patterns of purple acid phosphatase genes in *Arabidopsis* organs and functional analysis of AtPAP23 predominantly transcribed in flower. Plant Mol Biol **59:** 581–594

**Zimmerman P, Regrierer B, Kossmann J, Amrhein N, Bucher M** (2004) Differential expression of three purple acid phosphatases from potato. Plant Biol **6:** 519–528